What Makes a Solar Flare?

--or--

What the Photospheric Magnetic Field Can Tell You, and what Statistics Can't

K. D. Leka
Colorado Research Associates Div.,
NorthWest Research Associates, Inc.

With: **Graham Barnes**, *CoRA/NWRA*
Don Mickey, *U. Hawai'i*
Mees Solar Observatory Observing Staff

- **Using photospheric magnetic field data to predict solar flares**
- **The statistical tests: is there anything there?**
- **Some comments on recent work by other groups.**
- **Using IVM "Survey" Data.**
- **Future: the chromosphere.**

This work was carried out at the Colorado Research Associates Division of NorthWest Research Associates, Inc., with data from the U. Hawai`i Mees Solar Observatory. Funding from the Air Force Office of Scientific Research is gratefully acknowledged under contracts F49620-00-C-0004 and F49620-03-C-0019

Q: Can we tell which active region will erupt?

"Observer's wisdom":
Active regions which are *large*, *complex*, and *evolving* have a greater likelihood of producing a solar flare.

- **Energetic events are usually associated with larger active regions; more area, more magnetic flux implies greater energy storage potential.**

- **The more magnetically complex a region is, the more it deviates from the lowest-energy state (and the more energy is available to be released in a flare). Active regions in the "δ" configuration are extreme examples of this.**

- **Evolving active regions, especially with new emerging magnetic flux, bring additional magnetic energy to the system and increase the magnetic complexity and energy available for flares.**

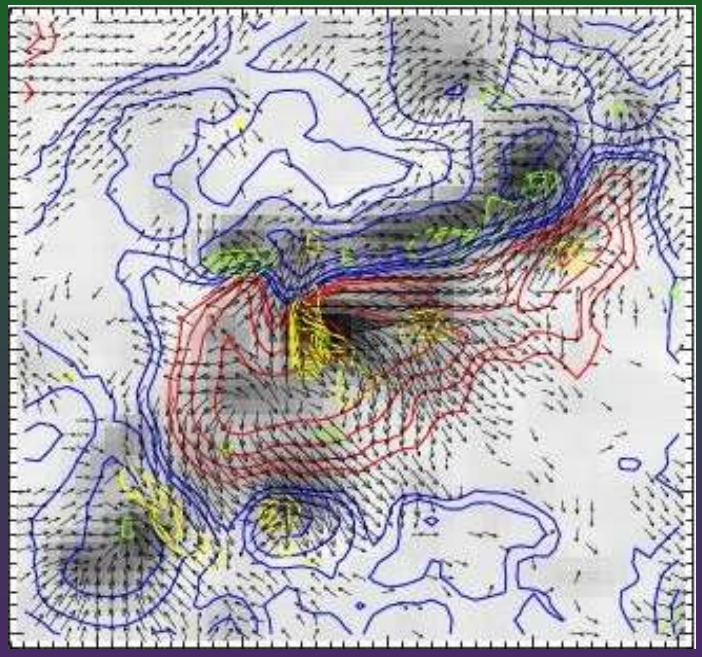

Q: Can we tell *when* an active region is going to erupt?

If the energy for energetic events is stored in, and released from, the magnetic field, that process *should* be observable in the active region's magnetic field configuration.

[the "*stress&release*" picture for solar flare energy]

- The photosphere provides the boundary condition for upper solar atmosphere; measuring the photospheric magnetic field should indicate the energy storage in the active region (with caveats).
- Numerous measures of magnetic complexity and energy storage can be derived from the photospheric field.
- A substantial body of prior work on various measures *vs*. solar flare activity have provided *initial targets* to consider.
- Many examples have been published showing changes in photospheric fields *associated with* solar events, *cf.* recent observations by Wang *et al.* 2002.

Demonstration Study of flare prediction on short time-scales using photospheric vector magnetic field data: Leka & Barnes *ApJ*, 2003 a, b

- Archive data from the Imaging Vector Magnetograph (U. Hawai`i) selected for well-observed flares and flare-quiet (but *flare-probable*) regions.
- Large field-of-view, few-minute temporal cadence, heliospheric magnetic vector utilized.
- Time sequences divided into *epochs*, each ending with either:
  - a GOES event, or
  - a data-gap, or
  - after more than an hour of continuous data (5-magnetogram min. imposed).
- Final tally: 10 flaring, 14 flare-quiet epochs.
- For each epoch, both the *mean* and *temporal variation* (slope) of the derived parameters are considered.

Table 2: Flaring and Flare-Quiet Epochs

NOAA AR Number	Start Time	End Time	Number Magnetograms	Event
8210	17:07	18:07	20	
8210	18:15	19:14	20	
8210	19:31	20:08	13	C2.8
8210	20:11	21:35	27	C2.6
8210	21:55	22:35	13	M1.2
8210	22:38	23:25	15	
8636	16:47	18:31	23	M1.1
8636	18:35	18:50	5	
8636	19:14	19:30	5	
8636	20:09	20:28	6	
8636	21:04	22:11	14	
8771	18:13	18:38	6	C1.6
8771	18:42	18:58	5	M2.0
8771	19:02	19:34	7	
8891	18:13	19:07	15	
8891	19:43	20:38	15	
8891	20:49	21:24	10	
9026	17:06	18:22	18	C3.8
9026	18:25	18:57	9	
9165	19:44	20:51	17	C7.4
9165	20:55	21:18	7	
0030	18:53	19:58	14	X3.0
0030	20:02	21:02	15	M1.8
0030	22:04	22:24	6	

What can be measured?

Examples:

horizontal gradients $$|\nabla_h B(x,y)| = \left[\left(\frac{\partial B}{\partial x}\right)^2 + \left(\frac{\partial B}{\partial y}\right)^2\right]^{\frac{1}{2}}$$

vertical current density $$J_z(x,y) = \frac{C}{\mu_0}\left(\frac{\partial B_y}{\partial x} - \frac{\partial B_x}{\partial y}\right)$$

measures of twist $$\alpha(x,y) = \frac{[\nabla_h \times \boldsymbol{B}_h]_z}{B_z}$$

"vertical" current helicity density $$h_c(x,y) = B_z \cdot [\nabla_h \times \boldsymbol{B}_h]_z$$

magnetic shear angles $$\Psi(x,y) = \cos^{-1}[\boldsymbol{B}^p \cdot \boldsymbol{B}^o / B^p\, B^o]$$

$$\psi(x,y) = \cos^{-1}[\boldsymbol{B}_h^p \cdot \boldsymbol{B}_h^o / B_h^p\, B_h^o]$$

Different parameterizations offer different weighting and sensitivity to measures of magnetic complexity and energy storage.

Each measure calculated at every well-measured point (x,y).

Images of continuum (top) and *Bz* (bottom, with +/- 100 G contours) of NOAA AR0030 (left), AR8636 (middle) and AR8891 (right); axes are in Mm. (black triangles are masked field stops).

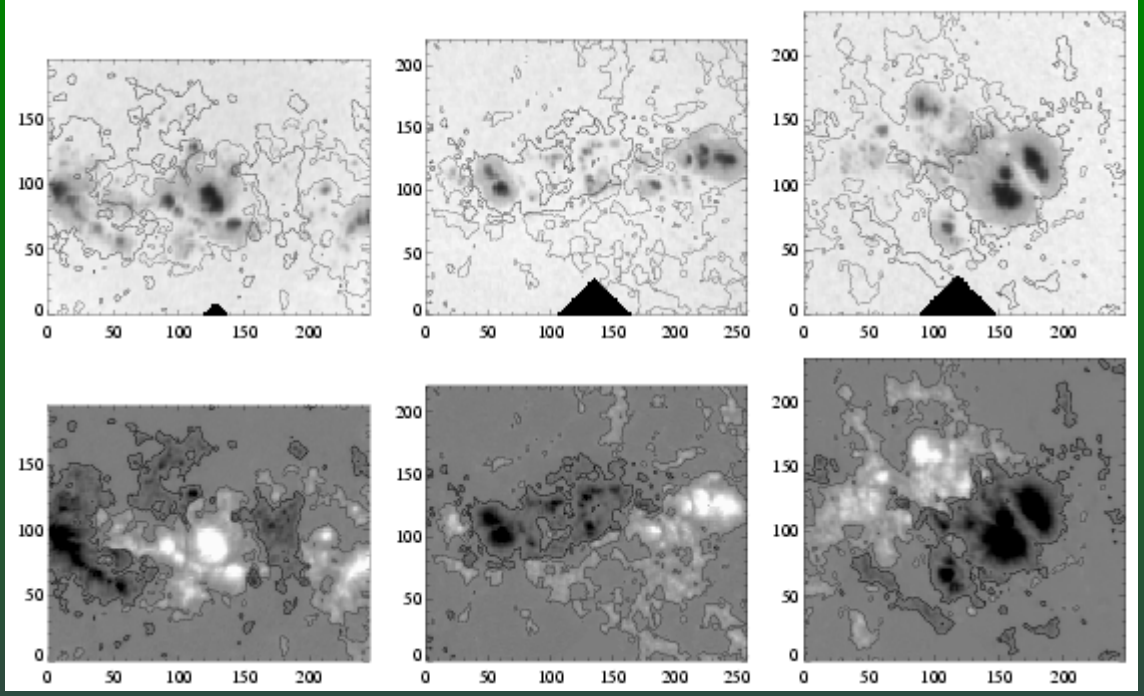

Magnetic state of the photosphere is described by quantities derived from the observed magnetic vector; the spatial distribution is parameterized using the moment analysis:

(plus totals and net quantities where appropriate)

$$\text{mean } \overline{x} = \frac{1}{n}\sum_i x_i$$

$$\text{standard deviation } \sigma = \left[\frac{1}{n}\sum_i (x_i - \overline{x})^2\right]^{\frac{1}{2}}$$

$$\text{skew } \varsigma = \frac{1}{n}\sum_i \left[\frac{x_i - \overline{x}}{\sigma}\right]^3$$

$$\text{kurtosis } \kappa = \frac{1}{n}\sum_i \left[\frac{x_i - \overline{x}}{\sigma}\right]^4 - 3.0$$

Goal: identify flare precursors, if any, measurable using photospheric vector magnetic field data.

Example: Magnetic Field Twist

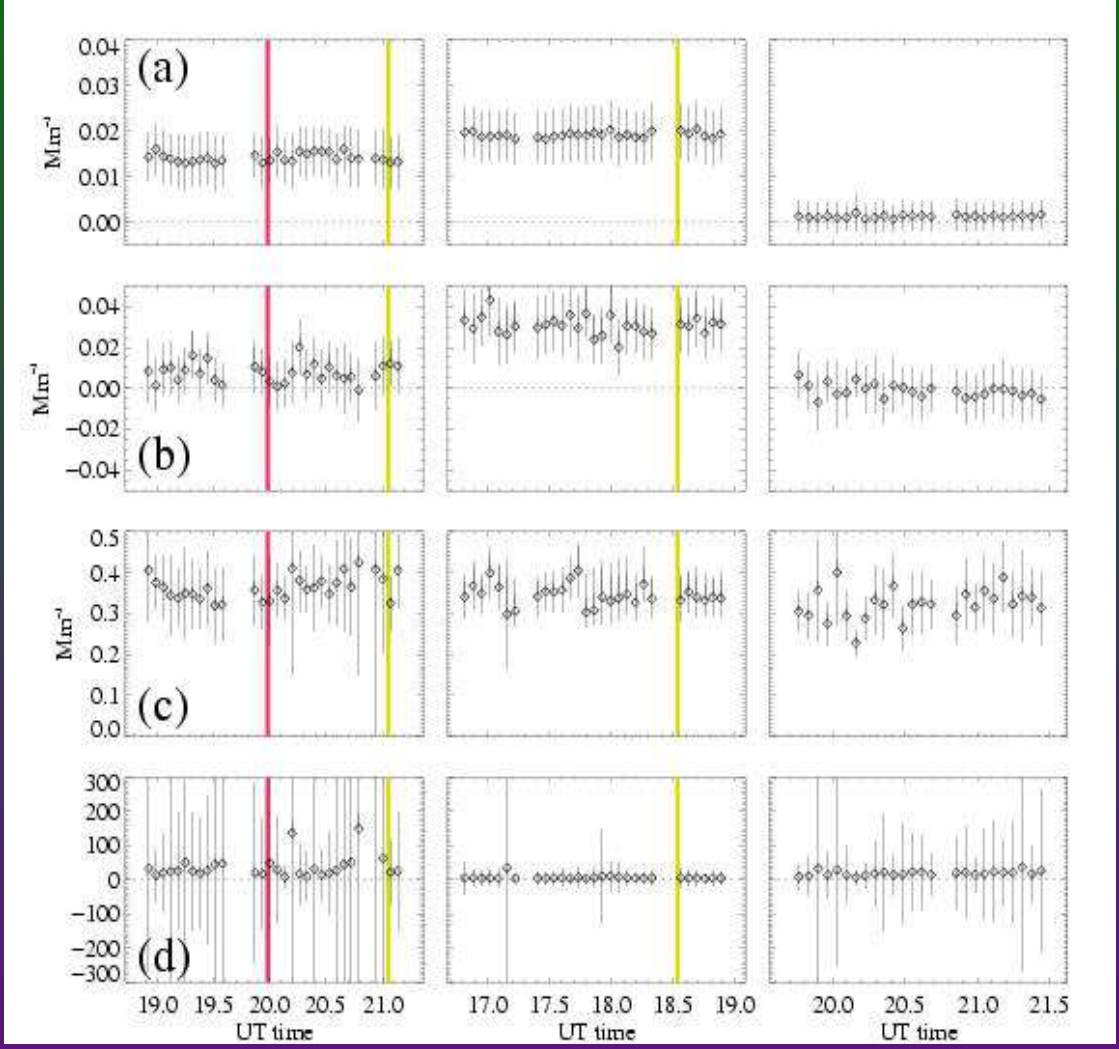

(a) the "best" force-free **α**, fit over entire active region, plotted as a function of time for the three target active regions relative to the start of an **X**- and two **M**-class flares.

(b) the mean of **α**(x,y)

(c) the standard deviation of **α**(x,y)

(d) the kurtosis of **α**(x,y)

Example: Magnetic Shear Angles

Consider four measures:

(a) 3-D shear angle Ψover entire active region

(b) 3-D shear angle Ψin NL areas

(c) Horizontal projection of shear angle ψ over entire AR

(d) Horizontal projection of shear angle ψ in NL areas.

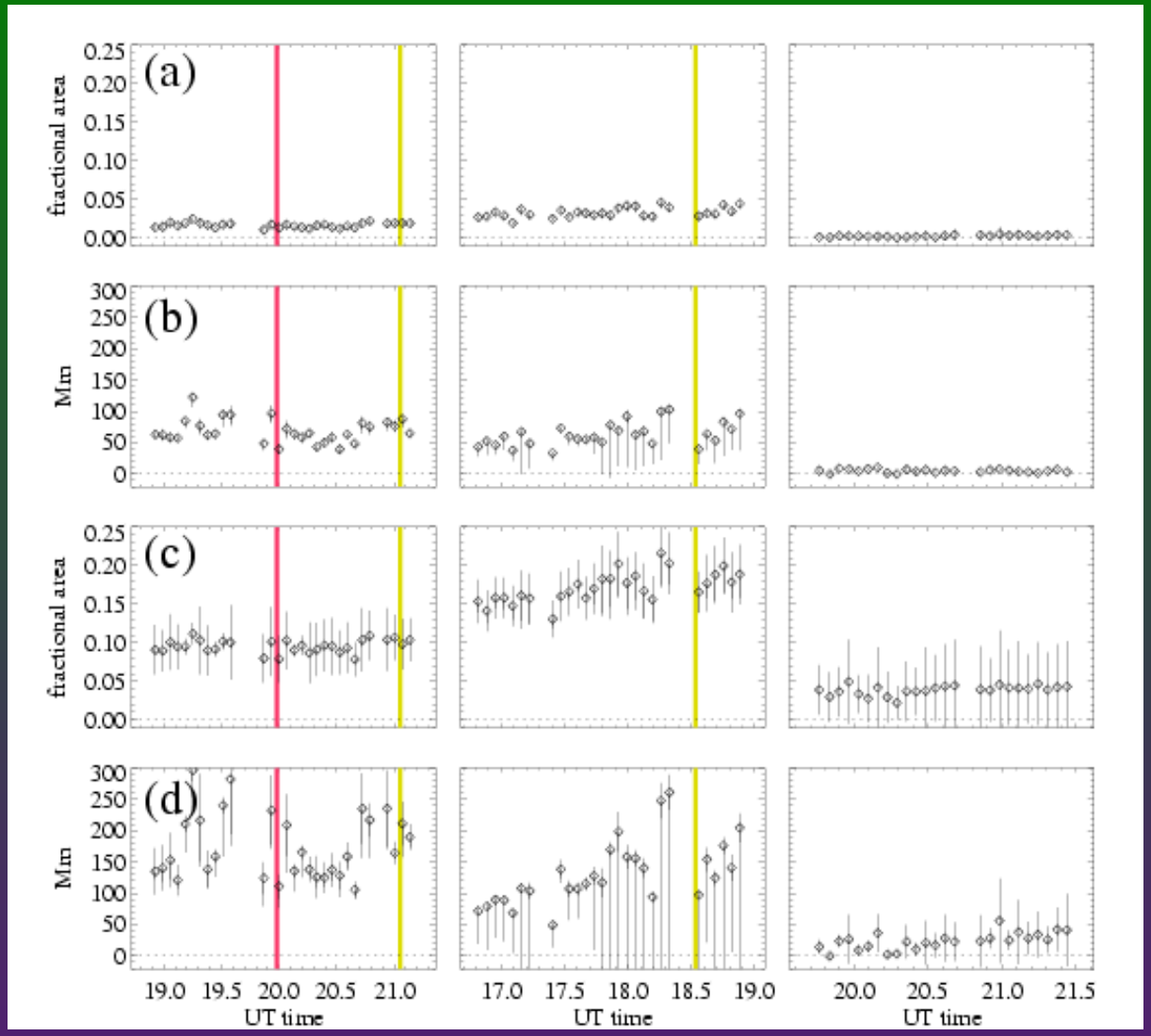

Thus far, little evidence that *any* single measure derivable from photospheric ***B*** implicates a stress/release mechanism in the photosphere.

No single silver bullet

Results from visual inspection of a gazillion parameters:

- **The majority show inconsistent results. Some display distinct rises/falls prior to flare events *when temporal windows are chosen subjectively*, e.g., σ(Jz), κ(Jz).**
- **Distinct overall flare-productivity signatures include: larger α_{ff}, greater extent of magnetic shear, larger Hc(net).**
- **In most cases, if a parameter exhibits a "significant" rise/fall prior to a flare, it also shows similar variations during flare-quiet epochs.**

Most importantly:

By requiring a flare-*unique* signature, numerous candidates are *removed from consideration* due to similar behavior during flare-quiet epochs.

Considering the behavior of a single parameter at a time in this manner can be very informative, but is inadequate to determine "What makes a flare?"

Q: Can samples from two populations (quiet, event-imminent) be distinguished?

Discriminant Analysis:

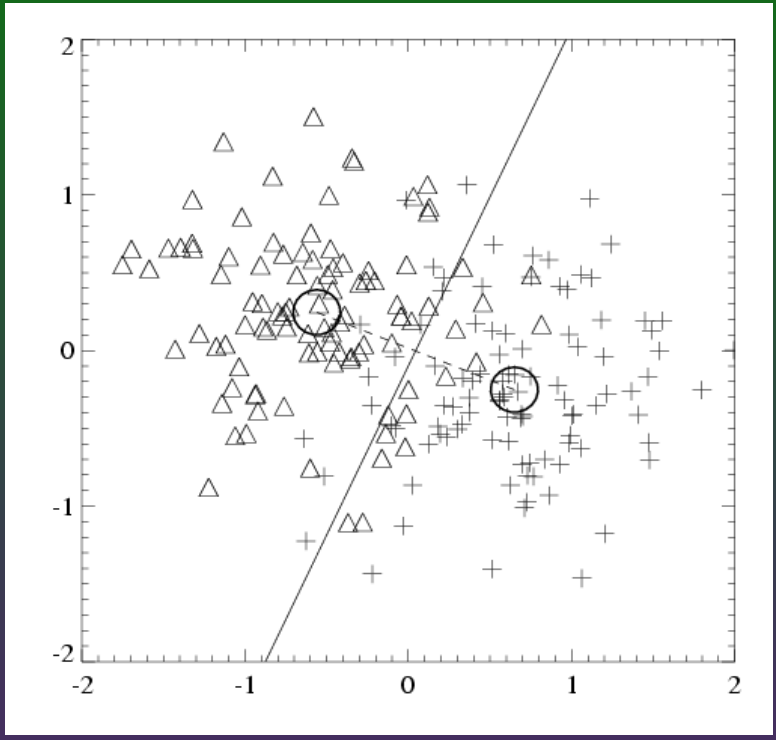

- Given measurements known to originate from two populations, a Discriminant Function divides parameter space into two regions.
- Maximizes correct "prediction".
- Simultaneously considers multiple variables.
- Magnitudes of DF coefficients give the relative predictive power of variables.
- Success rates constructed using "truth tables" or "classification tables"; ***these will always underestimate the errors***. Unbiased estimate possible using "n-1" approach.

Hotelling's T^2 test:

- Gives probability that samples come from distinct populations
- Essentially measures the distance between sample means, relative to their variances
- Even with a high probability of different parent populations, samples may have a large overlap.

Gentle Introduction, I:
Total Vertical Current *vs.* Total Magnetic Flux

Hotelling's T^2 test: probability that samples are from different populations: 0.327

Discriminant Function:

$$f = 0.0052 - 0.2891\langle \Phi_{tot} \rangle + 0.0673 \langle I_{tot} \rangle$$

Classification Table:

		predicted	
		flare	no flare
observed	flare	5	5
	no flare	6	8

Success from table: 0.542
Success from "n-1" approach: 0.375

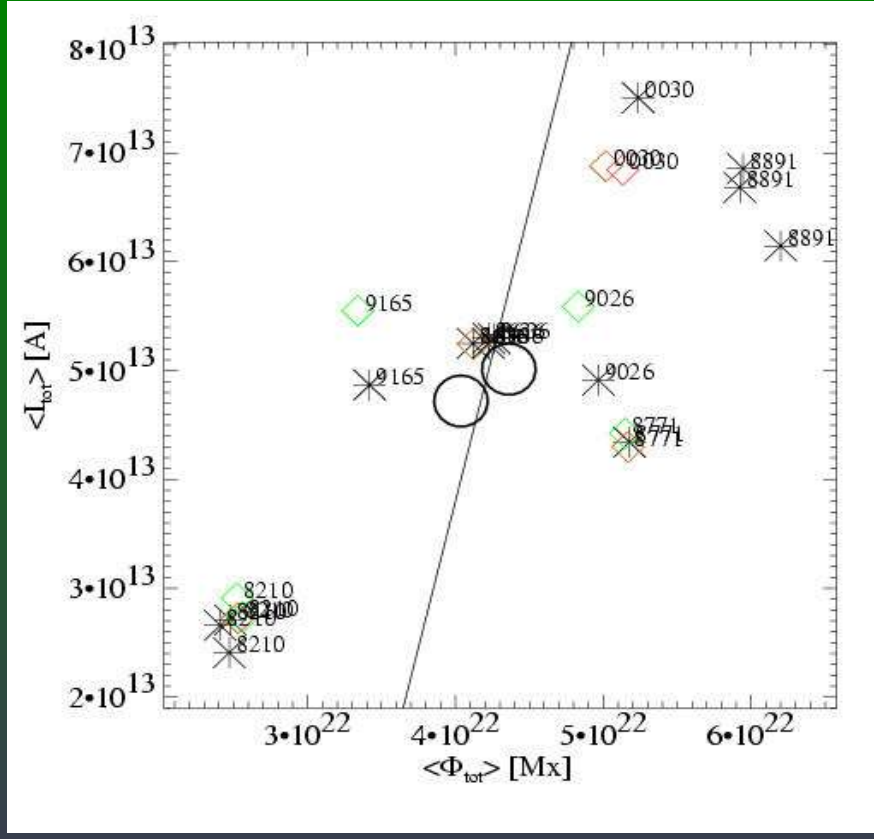

Parameter space and discriminant function for [$\langle \Phi_{tot} \rangle$, $\langle I_{tot} \rangle$]; ◇: flaring epochs with [C, M, X]-class flares. ✳: quiet epochs. ○: means of each sample. Solid line: discriminant function. Variables are correlated (although not related), which reduces the usefulness of the DF coefficients, and results in a non-perpendicular angle between it and the line connecting the two sample means.

Gentle Introduction, II:

Temporal variation of the kurtosis of the twist distribution *vs.* temporal variation of the standard deviation of the inclination angle distribution.

Hotelling's T^2 test: probability that samples are from different populations: 0.943

Discriminant Function:

$$f = 0.115 - 1.312\, d\sigma(\gamma)/dt + 1.434\, d\kappa(\alpha)/dt$$

Classification Table:

		predicted	
		flare	no flare
observed	flare	8	2
	no flare	4	10

Success from table: 0.750
Success from "n-1" approach: 0.750

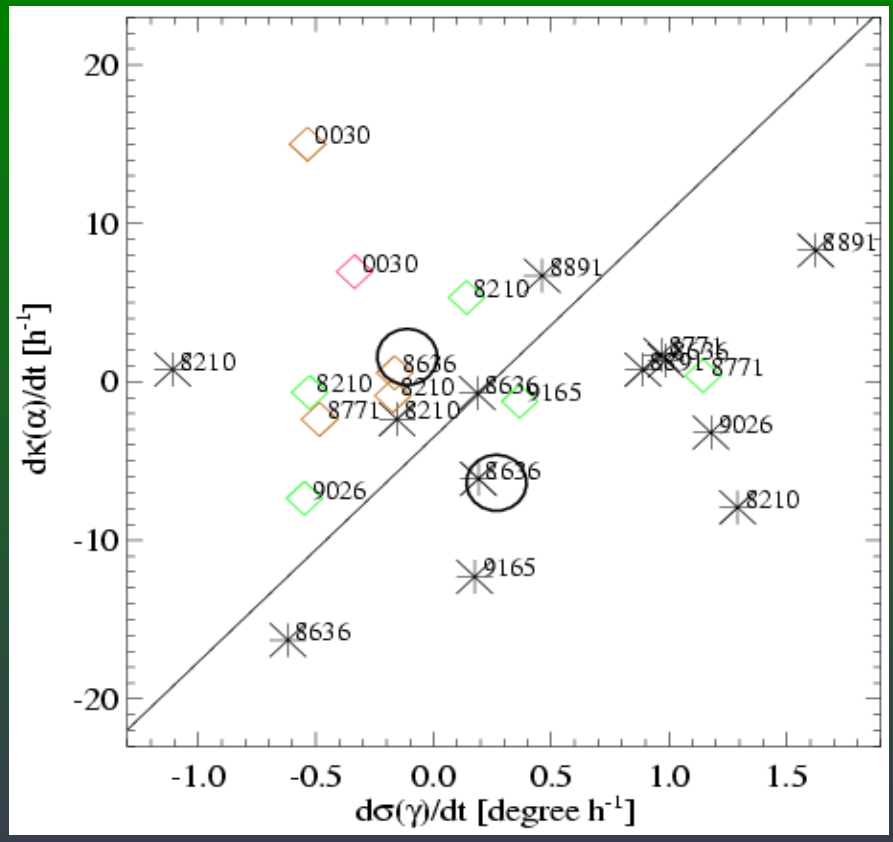

Parameter space and discriminant function for [dσ(γ)/dt, dκ(α)/dt]. ◇: flaring epochs with [C, M, X]-class flares. ✳: quiet epochs. ○: means of each sample. Solid line: discriminant function. Variables are not correlated, which results in a DF perpendicular to the two sample means.

Discriminant Functions of more than two variables

- DF becomes a hyper-plane in parameter-space
- Small-number statistics: *results here are for demonstration only!*

Example: Two Two-variable DFs:

$f[\langle\ (\psi)\rangle\ , \langle\kappa(hc)\rangle]$, probability = 0.047

$f[\langle\ (Bh)\rangle\ , \langle\kappa(|\nabla Bh|)\rangle]$, probability = 0.625

Combine for a Four-variable DF:

$f = 0.327 - 8.574\langle\ (\psi)\rangle - 2.277\langle\kappa(hc)\rangle - 5.690\langle\ (Bh)\rangle + 7.479\ \langle\kappa(|\nabla Bh|)\rangle$

Hotelling's T^2 probability: 0.997

Classification Table:

		predicted: flare	predicted: no flare
observed	flare	8	2
	no flare	2	12

Success from table: 0.833

Success from "n-1" approach: 0.708

Example: Six-Variable Discriminant Function:

$$f = 1.021 - 11.098\,\langle\sigma(B_h)\rangle + 7.460\,d\overline{B_z}/dt + 8.330\,\langle\varsigma(J_z^h)\rangle - 3.829\,\langle\kappa(J_z^h)\rangle$$
$$- 7.718\,\langle A(\psi > 80^\circ)\rangle - 3.834\,d|\alpha_{ff}|/dt$$

Hotelling's T^2 probability: 0.999995

Classification Table:

		predicted	
		flare	no flare
observed	flare	10	0
	no flare	0	14

Success rate from table: 1.00
Success from "n-1" approach: 0.875

Perfect classification is possible with the data and variables considered here. This example is *not unique*: there are many other combinations which result in perfect classification tables and Hotelling T^2 probabilities *above* 0.999990.

A different tact: using photospheric magnetic field data for daily predictions of CME activity. Falconer *et al.* 2002 ApJ, 2003 JGR, AAS 2004.

- Derive magnetic complexity measures from archived daily MSFC photospheric magnetograms.
- Compare CME production in those active regions surrounding the time of the magnetogram to measures of non-potentiality and magnetic complexity.

Figure 3a from Falconer et al 2003: Correlation plots of values of LSS and LSG measured in 17 magnetograms. Each LSG value is the extent of the strong field main neutral line having line-of-sight field gradient steeper than 25 G/Mm. The vertical line in each panel marks the LSS (length of strong shear in main neutral line) threshold value at and above which the active region is expected to be CME productive in the ±2-day window. The threshold value of LSG for CME expectation is marked by the horizontal line in each panel. The points are for magnetograms of CME-productive active regions (*) and non-CME-productive active regions (◊). The two percentages in the upper right corner are the confidence level and success rate of the correlation of LSG with LSS; those in the lower right corners are for the correlation of LSS with CME productivity; those in the upper left corners are for the correlation of LSG with CME productivity.

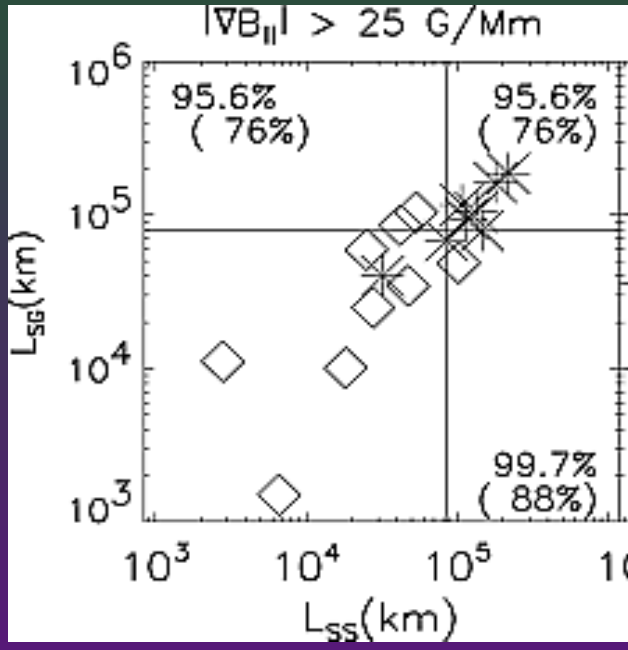

General comment concerning this work effort:

- Great to see a systematic comparison of CME-productive *vs.* CME-quiet ARs.
- The statistical approach is basically sound, but may not be optimized for forecasting.
- Is the few-day forecast useful? Probably, but usefulness limited for CME effects.

Issues I take with this research effort:

- **Selection effect imposed:** only bipolar active regions with *a single* strong neutral line and *sufficiently strong transverse fields* are included. Subjectively pre-selects for compact, strong-field but not particularly complex active regions. OK for science, not great for forecasting.
- **Using observed, not physical quantities:** Effects seen in line-of-sight magnetic field and the direction-ambiguous magnetic component transverse to the line of sight will *directly* depend on the observing angle to the active region. Basing any method on results that depend on the location of the active region is a red herring at best.

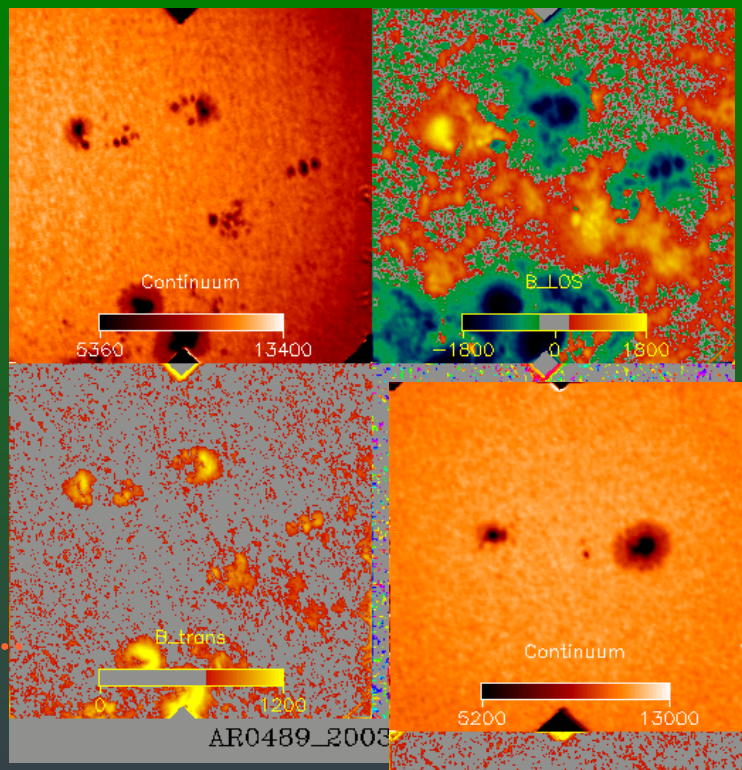

no...

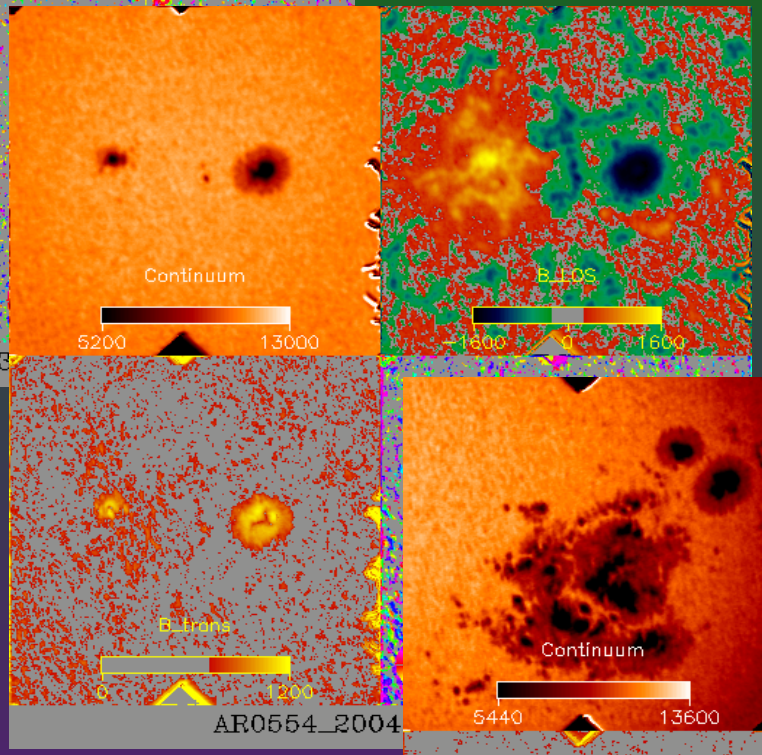

no...

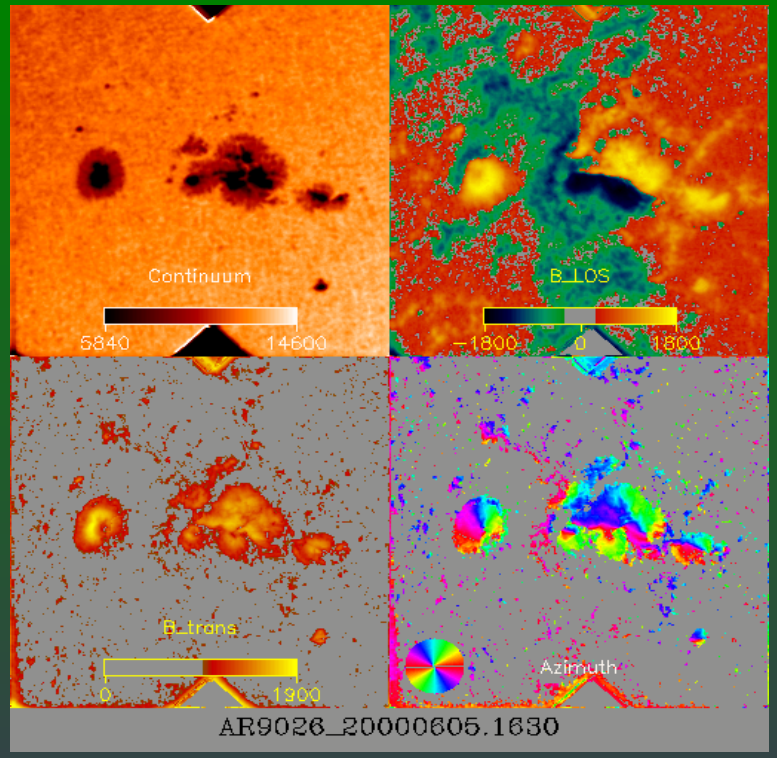

Yes.
But only one part of it.

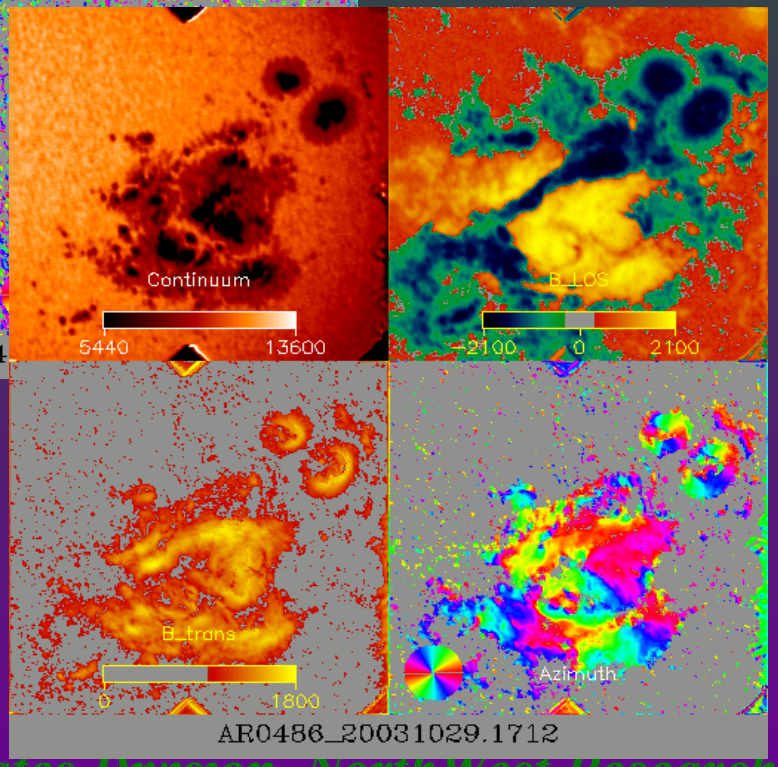

no....

Observed vs. Physical Quantities

➢To obtain physical quantities, one must transform the observed [*Bl, Bt,* ϕ] components to heliographic [*Bx, By, Bz*] via the ambiguity resolution.

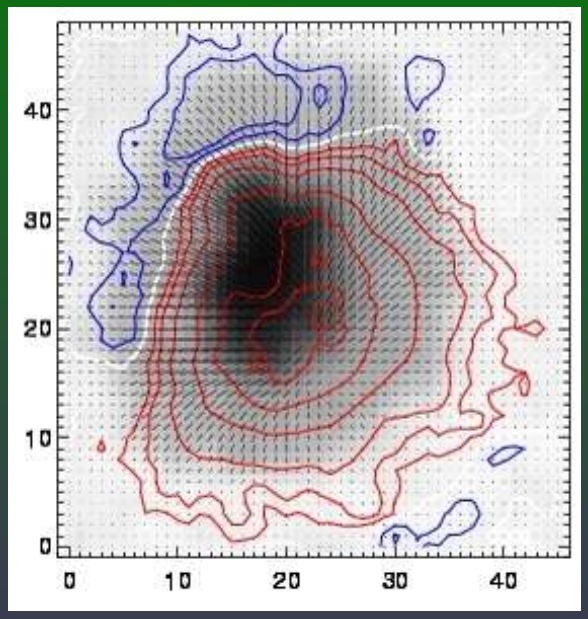

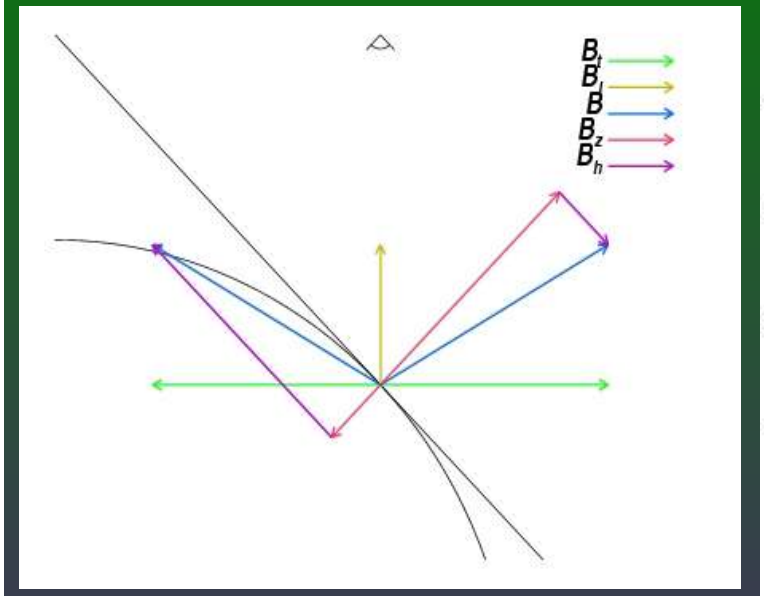

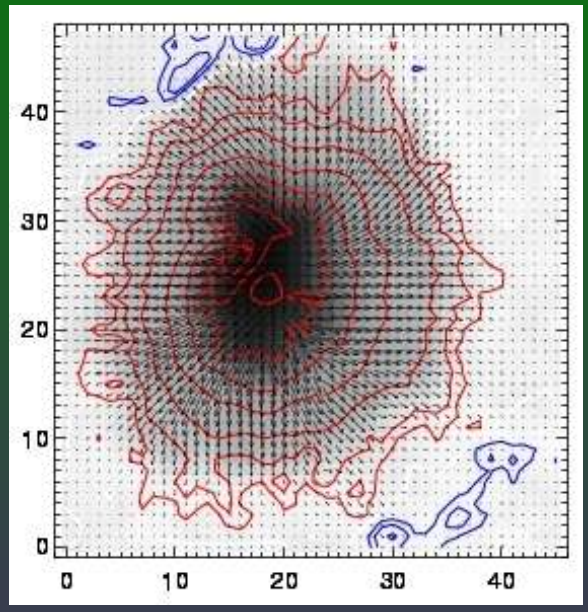

➢Potential field calculation *requires* the normal (*Bz*) component of the field, only available after ambiguity resolution and transformation. Neither "Lss" nor "Lsg" can be calculated without potential field.

➢Shear in the direction-ambiguous *Btrans* is only known if *45* < ψ < *135*; otherwise, it is still ambiguous (ψ > 135 == ψ < 45). "Lss" cannot be calculated without ambiguity resolution.

➢Contour integral for "Inet" only valid if *Bz* does not change sign; 100G contour of *Blos* does not guarantee this, *especially* in regions of strong *Btrans* at μ < 0.98. "Inet" , α cannot be calculated via contours of *Bl, Bt* .

Discriminant Analysis using IVM "Survey" data

- Utilize IVM "survey" database: daily single-shot vector magnetograms of every active region on the visible solar disk.
- Only selection criteria: $\mu > 0.5$ and $B > 500G$ somewhere in the magnetogram.
- A region was considered flare active/quiet if it did/did not produce a flare in the 24h post-magnetogram (the rule for now).
- Initial tally: 94 "Flaring", 382 "Flare-Quiet" data points.
- Same analysis approach as with the time-series data: parameterizations (moment analysis, summations) of physical quantities (*Bz*, *Jz*, α, etc.) derived spatially over the magnetograms. (temporal evolution no longer considered.)

ONE-DAY SAMPLE of SURVEY DATA

Magnetogram		NOAA AR	Flare Start		Peak
Day	UT Time	Number	Day	Time	X-Ray Flux
20020107	1734	09773	20020107	2049	C2.9
//	//	//	20020107	2243	C2.8
//	//	//	20020108	1255	C2.5
20020107	1740	09761	...	...	...
20020107	1745	09772	...	...	...
20020107	1750	09767	20020108	1713	C7.2
20020107	1754	09771	...	...	...

First Look at the DA Results with Survey Data

- **Most discriminating single variable:**
  Total "vertical" Current Helicity:
  $H_c = \sum |B_z(x,y) \cdot J_z(x,y)|\, dA$
  T^2 probability: 1.000; Success rate: 0.836

		predicted	
		flare	no flare
observed	flare	41	53
	no flare	40	342

- **Least discriminating: Seeing! (really!)**
  Next: Area of strong horizontal magnetic shear,
  $A(\psi > 45\text{deg})$.
  T^2 probability: 0.758; Success rate: 0.242

		predicted	
		flare	no flare
observed	flare	66	28
	no flare	333	49

- **Example of a good 2-variable DF:**
  Φ_{TOT} *vs.* $\sigma(B_z(x,y))$
  T^2 probability: 1.000; Success rate: 0.742

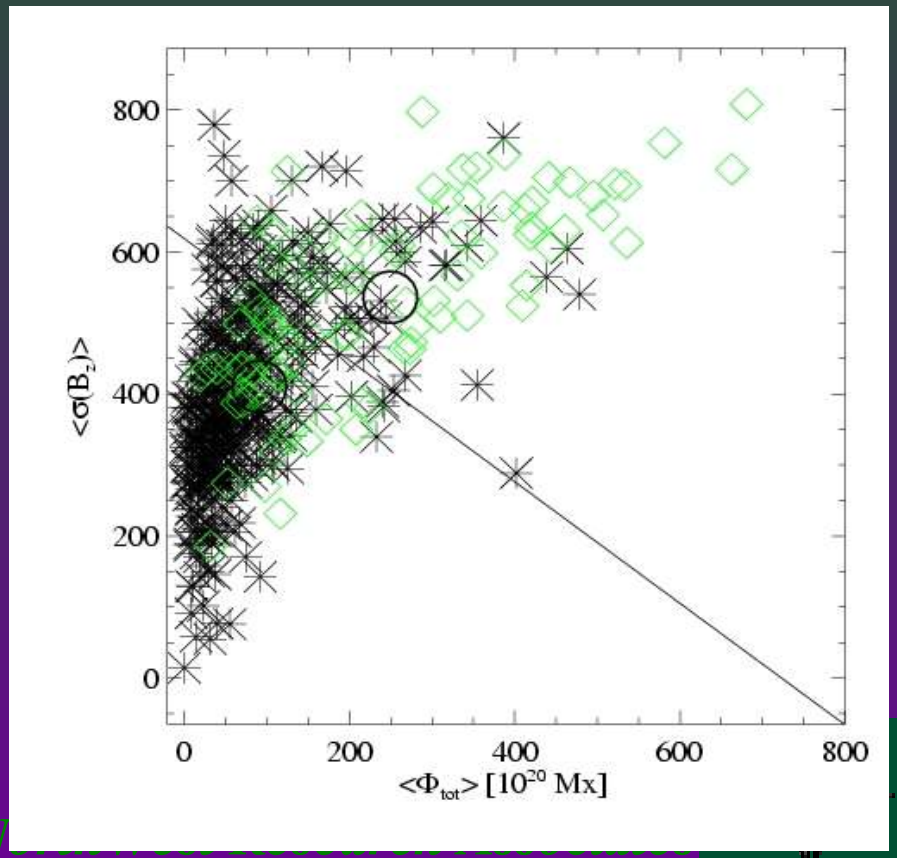

"Statistics are like bikinis: they show a lot but hide the important stuff"....

A Closer Look, I: Unequal Population Sizes

- Consider two populations: N1=A + B, and N2=C+D.

		PREDICTED	
		flare	no flare
OBSERVED	flare	A	B
	no flare	C	D

- Possible Rules for DA:
  - Minimize overall mis-classification, *i.e.* min(B+C). (our approach for large sample size, e.g., survey data; accounts for unequal population sizes)
  - Require equal errors of both types, *i.e.* B = C. (Falconer *et al.*'s approach)
  - Produce errors proportional to the population sizes, *i.e.* B/(A+B) = C/(C+D). (our approach for small sample sizes: no *a priori* assumption about population sizes)
- If N1=N2, all three produce the same result.

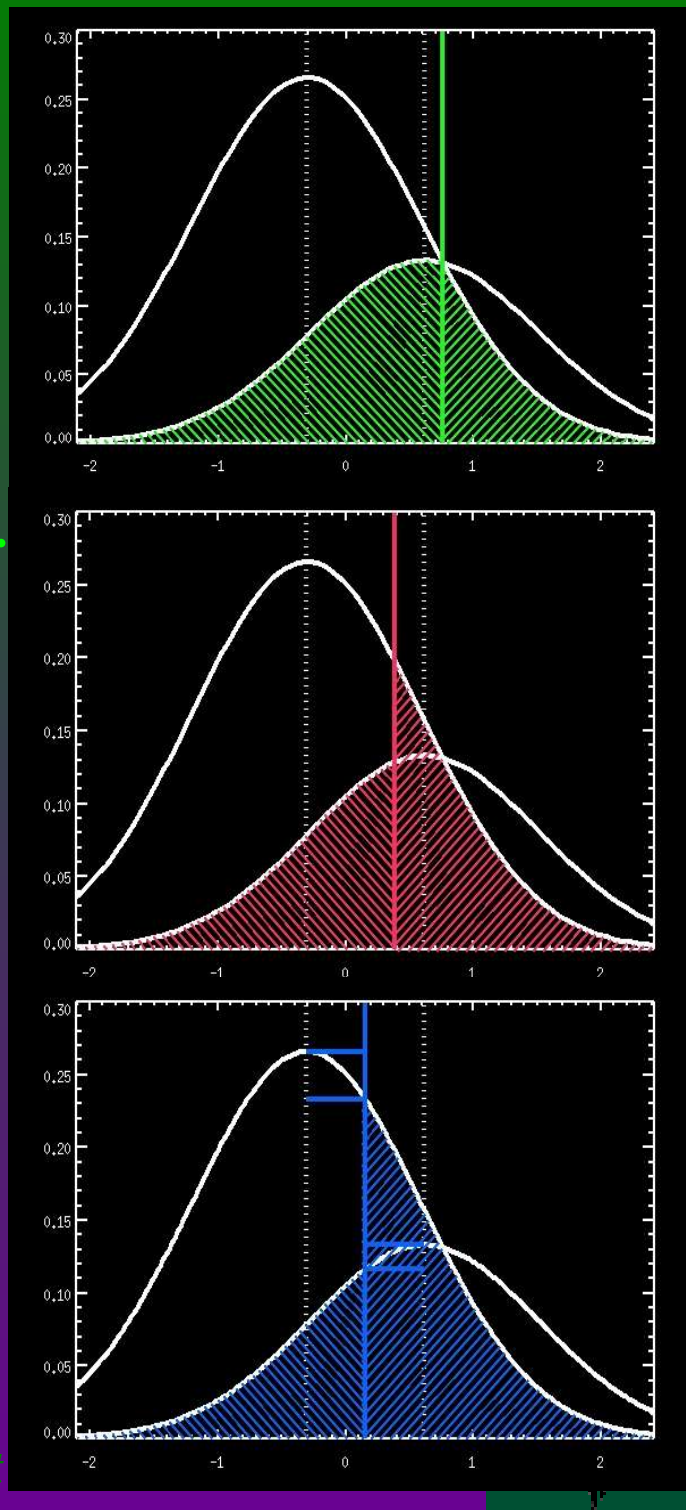

- **Why is this important?** ***It's what the Sun does.***
  - **80%** of Active Regions ***do not produce a flare C-class or larger*** in the 24 hr following a magnetogram. Two relevant implications:
  - **FIRST**, even with no information, one can achieve an 80% success rate by predicting nothing will ever flare. *E.g.*, **seeing**:

		PREDICTED flare	PREDICTED no flare
OBSERVED	flare	0	94
	no flare	0	382

Success rate: 0.802

  - **SECOND**, accounting for unequal population sizes changes the outcome of the DA.

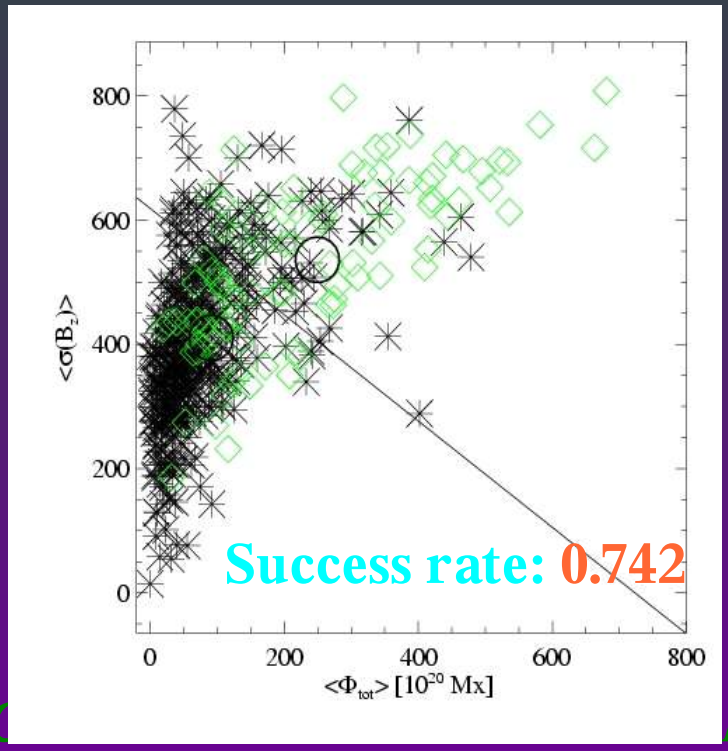

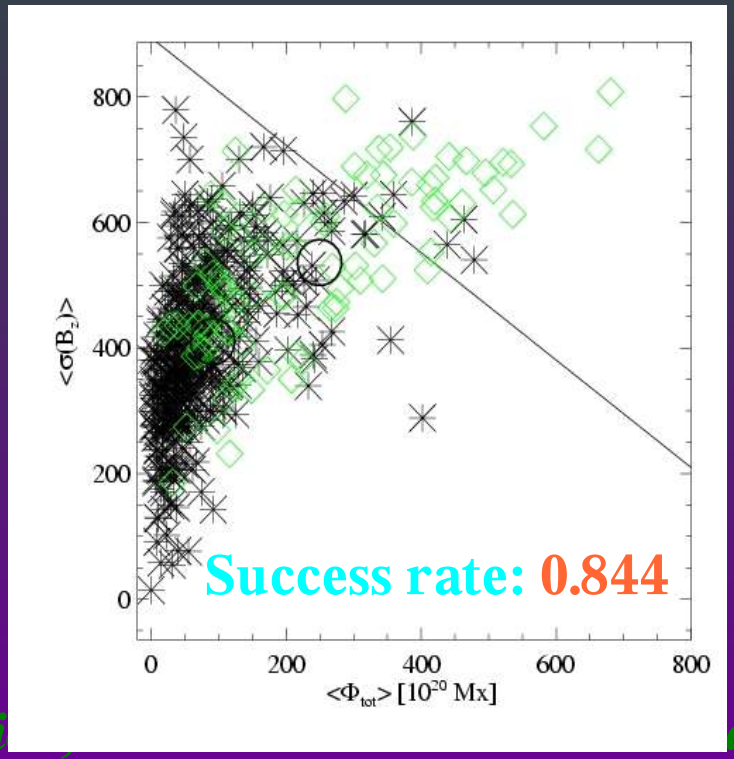

A Closer Look, II: Unequal Population Distributions

- This is also *what the Sun does*: populations do not necessarily have the same covariance matricies (as assumed for a linear DA).
- To accommodate this: non-linear DFs

How well can we do?
Multiple Variables Simultaneously

- The Big, the Bad *and* the Ugly
- With Statistically Significant Samples:
  - No perfect classifications
  - Can finally do "all-variable" DF.

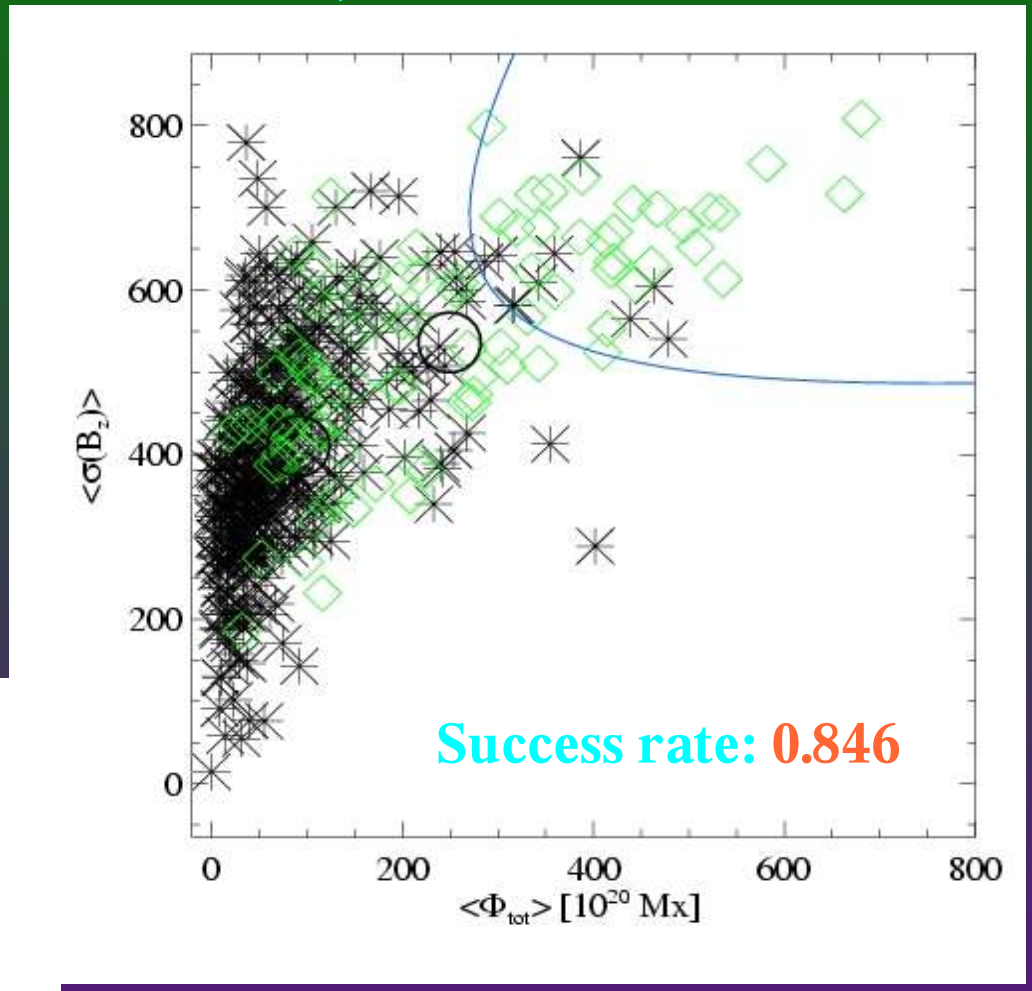

Effects of Adding Variables
(Unequal-Population, Quadratic DFs)

# Variables		classification success rate
1	Φ_{tot}	0.8319
2	add..$\varsigma(\nabla_h(B_h))$	0.8340
3	add.....$\varsigma(J_z)$	0.8424
4	add.....$\kappa(\gamma)$	0.8613
5	add .....$\sigma(E_e)$	0.8760
89	add ..the rest	0.8824†

†: Linear only: Quadratic DF not available for this many variables, yet.

Are We Done Yet? No.

A Closer Look, III: Non Gaussian Population Distributions

- Both linear, non-linear DFs *assume* the populations are Gaussian.
- The Sun rarely cooperates *(it's what the Sun does*, again).
- Explicitly accounting for non-Gaussian distributions is tough (and we've not yet tackled it).

Intermediate Conclusions:
DISTINCTION is *not* the same as PREDICTION

- Statistically easy to differentiate between flaring, non-flaring populations using information from the photospheric vector magnetic field. *HOWEVER* this may only translate to a moderate predictive capability.
- The distributions of variables holds information about active region formation and evolution, especially as related to energetic event production *AND* taking into account this information may improve predictive capability.
- We have not found a unique set of parameters from vector magnetic field data which *guarantees* an energetic event, *AND* non-Gaussian distributions, *etc.* may mask their existence, *BUT STILL* we can begin to distinguish necessary *vs.*, sufficient conditions for energetic events, and provide critical-level/thresholds.

A Closer Look, IV: Looking for Keys under a Streetlight.

- The photosphere's magnetic plasma is forced: $J \times B \neq 0$, meaning the currents and complexity measured in the photosphere may not relate directly to the state of the plasma where magnetic reconnection occurs, in the chromosphere/corona.
- However, the photosphere is where the data are. Until now.
- In Autumn 2003, *years* of thought & labor (& money!) paid off: the IVM filter wheel was installed; data now obtained in both photospheric FeI and chromospheric NaI D1 line *with minimal delay*
- Chromospheric vector magnetic field observations, where $J \times B = 0$, are now being obtained in both "survey" and "time-series" modes
  - Time-series pre-event data are sparse and will stay that way for a while as we enter solar minimum.
  - "Survey"-mode data are accumulating; next year we plan to begin investigating that database.
  - Some preliminary results are exciting:

Determining the Magnetic Free Energy

Magnetic virial theorem: only applies if field is force-free (i.e., in the chromosphere/corona)

AR 10621:

- Ef: 4.30 +/- 4.02 $\times$ 10^{32} erg.
- Consistent with zero free energy.
- Simple AR; relatively few points with 3- field
- Consistent w/ lack of activity.

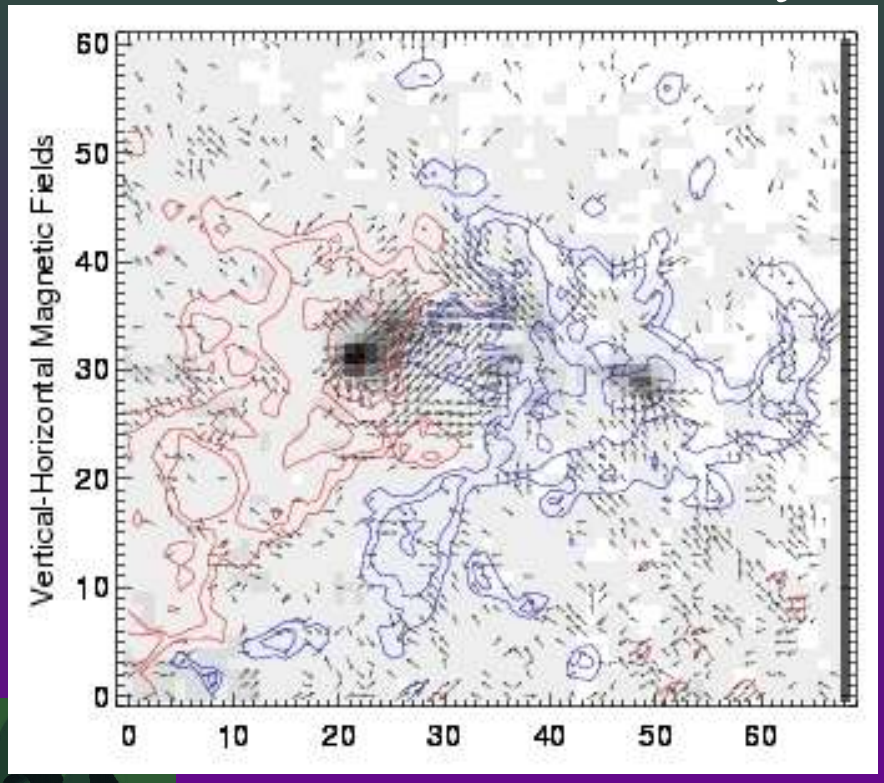

AR10468:

- Ef: 8.66 +/- 2.3 $\times 10^{33}$ erg.
- Very large amount of free energy.
- Large AR; very complicated but adequate 3- fields.
- Consistent with high activity level.

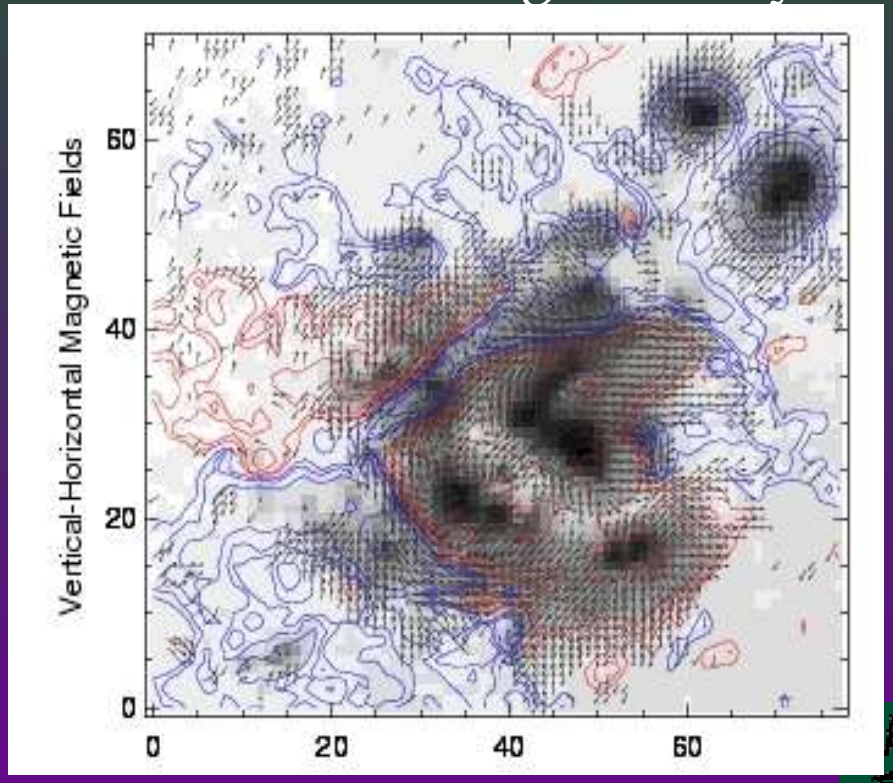

This, that, and the other... Final Comments.

- Examining time-series magnetic field data for changes relative to flares or CMEs can be an informative first step. But it's far from our goal of characterizing the pre-event solar atmosphere.
- The requisite approach includes event-quiet samples as a control group for statistical tests of the null hypothesis. Various groups are starting to embrace this.
- For true short-window pre-flare prediction, statistically significant samples of vector field data, possibly chromospheric, are required. Not available yet.
- In the meantime, we *demonstrate* Discriminant Analysis on physically meaningful parameters derived from photospheric time-series data, and *apply it with attention to its limitations* to a significant sample of daily magnetograms.
- Our effort is ongoing with various paths planned. Our ears are open for suggestions, ideas, and concerns.